# Self-Tuning Control of a Nonlinear Model of Combustion Instabilities

Miroslav Krstic, Ashish Krupadanam, and Clas Jacobson, *Member, IEEE*

***Abstract*—We present a self-tuning scheme for adapting the parameters of a proportional integral (PI) controller proposed by Fung and Yang for stabilization of a Culick-type model of nonlinear acoustic oscillations in combustion chambers. Our adaptation criterion is Lyapunov-based and its objective is the regulation of nonlinear pressure oscillations to zero. We focus on a two-mode model and first develop a design based on an assumption that the amplitudes of the two modes are available for measurement. The adaptation mechanism is designed to stabilize both modes and prevent the phenomenon observed by Candel and coworkers whose adaptive controller stabilizes the first but (under some conditions) apparently destabilizes the second mode. We also prove that the adaptation mechanism is robust to a time delay inherent to the actuation approach via heat release. In order to avoid requirements for sophisticated sensing of the mode amplitudes needed for feedback, we also develop an adaptation scheme which employs only one pressure sensor. In order for the adaptation scheme to be implementable, it is also necessary to know the control input matrix of the system. Rather than performing a linear ID procedure with input excitation, we propose a simple nonlinear ID approach based on limit cycles (internal excitation) which exploits the quadratic character of the nonlinearities. Simulations illustrate the scheme's capability to attenuate limit cycles and its robustness to magnitude- and rate-saturation of the actuator.**

***Index Terms*—Adaptive control, averaging, combustion control, Galerkin approximation, nonlinear acoustics.**

## I. Introduction

ACOUSTIC instabilities in combustion chambers have been a significant problem in the design of propulsion systems. The instabilities are generated by the feedback coupling between the acoustic resonances and the heat release of the combustion processes. The instability problem can be alleviated by changing the design of the chamber to either increase the damping in the system or reduce the coupling between flow oscillations and unsteady combustion. However, these passive techniques are neither systematic, nor robust in the face of changes in operating conditions or aging. For this reason, active control of combustion instabilities is a field that has grown in significance over the last few years, and already seen remarkable advances [1]–[4], [7]–[13], [16]–[18], [20], [22], [24], [25]. With respect to the actuation mechanism, it is possible to categorize the control methods into two groups: 1) mechanical methods which use loudspeakers or moving bodies (less feasible for propulsion systems because they require a large amount of power) and 2) methods which use a secondary supply of fuel (more promising for propulsion systems). Another categorization, to experiment-based and model-based control, was given by Fleifil *et al.* [8] who note that, in some of the experiment-based designs [3], [4], [11], [16]–[18], [22], the suppression of the primary pressure peak is accompanied by excitation of secondary peaks.

Combustion instabilities take a form of nonlinear oscillations—limit cycles. A nonlinear model of acoustic waves in a combustion environment has been developed by Culick [5] (a large volume of other literature on this topic also exists which we do not attempt to review here). Reduced-order models obtained by Galerkin projection, averaging, and truncation to the first few modes were studied by Culick and coworkers (see, e.g., [21] and references therein) and shown to give a satisfactory qualitative match with experimental results.

Fung and Yang [9] and Fung *et al.* [10] were the first to develop control-oriented extensions of Culick-type models and to propose the use of various control techniques motivated by their models. In particular, Fung and Yang [9] studied in detail the effect of PI compensators and showed that they can achieve stability in at least two-mode truncations of their models.

The selection of gains in Fung and Yang's PI controller [9] requires the knowledge of the model parameters. If these parameters are not known or change with operating conditions, it is possible that the mistuned controller makes one or more modes unstable. The need to use adaptation was first recognized by Billoud *et al.* [3] who used a least mean square (LMS) adaptive filter to suppress pressure oscillations. Even though not model-based, their approach was experimentally successful. However, they did observe that the suppression of the first mode is (under certain conditions) accompanied by the destabilization of the second mode.

In this paper we build upon the model-based control results of Fung and Yang [9] and develop a technique for self-tuning of the parameters of a PI controller to ensure the stabilization of both the first and the second mode. We achieve this by pursuing a Lyapunov-based adaptation criterion which takes both modes into account.

Manuscript received February 21, 1997; revised December 23, 1997. Recommended by Associate Editor, M. Jankovich. This work was supported in part by a gift from the United Technologies Research Center, the Office of Naval Research, the Air Force Office of Scientific Research, the University of California Energy Institute, and by the National Science Foundation.

M. Kristic is with the Department of Applied Mechanics and Engineering Sciences, University of California-San Diego, La Jolla, CA 92093 USA.

A Krupadanam is with the Department of Mechanical Engineering, Massachusetts Institute of Technology, Cambridge, MA 02139 USA.

C. Jacobson is with UTRC, East Hartford, CT 06108 USA.

Publisher Item Identifier S 1063-6536(99)05856-X.

1063–6536/99$10.00 © 1999 IEEE

We first develop adaptation laws under the assumption that the amplitudes of the modes are available for measurement. The derivation and the proof of stability in Section III are followed by simulations in Section IV. In Section V we establish robustness of this scheme to a time delay inherent in the actuation mechanism. Then in Section VI we relax the assumption from Section III and derive update laws which do not require the modal amplitudes but only pressure measurements from a single sensor in the combustion chamber. In Section VII we propose a *nonlinear* identification procedure for estimating the input matrix of the system necessary for implementation of the adaptive scheme in Sections III and VI. Instead of performing a complicated linear identification of this matrix, we exploit the quadratic character of the model nonlinearities and estimate the matrix from steady-state limit-cycle data. Section VIII presents a simulation study on the nonaverage model. In the absence of actuator limitations, our adaptive scheme drives both modes to zero. When the actuator is both magnitude- and rate-saturated, our adaptive controller only reduces the size of the limit cycle. To prevent parameter drift, we employ update law leakage which stops the drift without increasing the size of limit cycles and without requiring *a priori* knowledge of a set of stabilizing parameter values.

## II. Controlled Modal Model

The mass, momentum (inviscid), and energy conservation equations for a two-phase mixture in a combustor are [6]

$$\frac{\partial \rho}{\partial t} + v_g \cdot \nabla \rho = \mathcal{W} \tag{1}$$

$$\rho \frac{\partial v_g}{\partial t} + \rho v_g \cdot \nabla v_g + \nabla p = \mathcal{F} \tag{2}$$

$$\frac{\partial p}{\partial t} + \bar{\gamma} p \nabla \cdot v_g + v_g \cdot \nabla p = \mathcal{P} \tag{3}$$

where $\rho$ is the local density of the mixture, $v_g$ is the local velocity of the gas phase, $p$ is the local pressure, $\bar{\gamma}$ is the averaged ratio of specific heats, and $\mathcal{W}$, $\mathcal{F}$, and $\mathcal{P}$ account, respectively, for the exchange of mass, momentum, and energy (including the heat of combustion) between the fuel and the gas. The energy equation is written with the pressure as the dependent variable using the perfect gas law. From the above equations, after separating $v_g$, $\rho$, and $p$ into the steady and fluctuating components, Culick [5] derives a wave equation with associated boundary conditions

$$\nabla^2 p' - \frac{1}{\bar{a}^2}\frac{\partial^2 p'}{\partial t^2} = h + h_c \tag{4}$$

$$n \cdot \nabla p' = -f - f_c \tag{5}$$

where $p'$ is the pressure fluctuation and $\bar{a}$ is the speed of sound in the mixture. The quantities $h$ and $f$ accommodate all influences of acoustic motions, mean flow, and combustion response, under conditions without external forcing. The terms $h_c$ and $f_c$ account for the effects of the control inputs. Fung *et al.* [10] have derived the relationship between the mass flow rate of the injected secondary fuel $\dot{m}_{\rm in}$ and the source term $h_c$ (we briefly review their derivation in this section keeping only details indispensable for our presentation). The distributed control action of the secondary fuel is approximated by an assembly of $M$ point actuators, as in Fig. 1, and $h_c$ is given by [10]

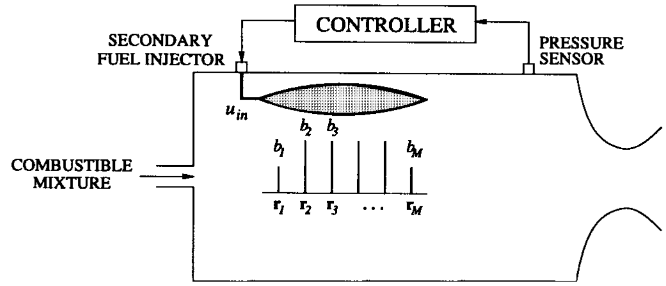


Fig. 1. Diagram of the feedback control system with distributed actuation via secondary fuel.

$$h_c(\mathbf{r},t) = -\sum_{k=1}^{M} b(\mathbf{r}_k) u_{\rm in}(t-\tau(\mathbf{r}_k))\delta(\mathbf{r}-\mathbf{r}_k) \tag{6}$$

where $b_k = b(\mathbf{r}_k)$ is the spatial distribution of the actuator output, $\tau_k = \tau(\mathbf{r}_k)$ is the time delay relative to the moment of injection for the $k$th point actuator, $\delta(\cdot)$ is the Dirac delta function, and $u_{\rm in}$ is a scaled version of the mass flow rate of the secondary fuel

$$u_{\rm in} = \frac{\bar{R}\Delta H_c}{\bar{a}^2 \bar{C}_v}\frac{\partial \dot{m}_{\rm in}}{\partial t} \tag{7}$$

where the coefficient $\bar{C}_v$ is the constant volume specific heat of the fuel mixture, $\Delta H_c$ is the heat of combustion of the fuel, and $\bar{R}$ is the gas constant of the mixture. As the source terms in (4) and (5) are treated as small perturbations to the acoustic field, the solution can be approximated by

$$p'(\mathbf{r},t) = \bar{p}\sum_{n=1}^{\infty} \eta_n(t)\psi_n(\mathbf{r}) \tag{8}$$

within second-order accuracy. The quantity $\psi_n$ is the normal mode function satisfying

$$\nabla^2 \psi_n + k_n^2 \psi_n = 0 \tag{9}$$

$$n \cdot \nabla \psi_n = 0. \tag{10}$$

Pure longitudinal oscillations in a uniform chamber give $\psi_n = \cos(n\pi z/L)$. The set of ordinary differential equations that represents the amplitudes of each mode obtained from (4), (8), and (9) via Galerkin projection is

$$\ddot{\eta}_n + \omega_n^2 \eta_n + \sum_{i=1}^{\infty}(D_{ni}\dot{\eta}_i + E_{ni}\eta_i) + \sum_{i=1}^{\infty}\sum_{j=1}^{\infty}(A_{nij}\dot{\eta}_i\dot{\eta}_j + B_{nij}\eta_i\eta_j) = U_n(t) \tag{11}$$

(see Culick [5] for the expressions for the $A, B, D, E$-coefficients), where $E_n^2 = \iiint \psi_n^2\, dV$ and the control input to the $n$th mode is

$$U_n(t) = \frac{\bar{a}^2}{\bar{p}E_n^2}\sum_{k=1}^{M} b(\mathbf{r}_k)\psi_n(\mathbf{r}_k)u_{\rm in}(t-\tau(\mathbf{r}_k)). \tag{12}$$

When we use no control, i.e., $u_{\rm in}=0$, which implies $U_n=0$, the system (11) has an unstable linearization and, due to the quadratic terms, for realistic values of the parameters, the solutions converge to a periodic orbit, as shown and discussed in Paparizos and Culick [21] and the references therein. The purpose of active control is to add feedback terms in $\eta_i$ through $u_{\rm in}$ to stabilize the system (11), (12). To a reader with experience in control theory it is obvious that this is a very difficult problem because 1) the control input $u_{\rm in}$ drives the system through time delays; 2) various coefficients in (11) and (12) cannot be assumed to be known accurately; and 3) the control $u_{\rm in}$ cannot apply feedback of $\eta_i$ but only a feedback of a variable that is physically measurable, such as, for example, the instantaneous pressure

$$y(t)=p'(\mathbf{r}_s,t)=\bar{p}\sum_{n=1}^{\infty}\eta_n(t)\psi_n(\mathbf{r}_s) \tag{13}$$

where $\mathbf{r}_s$ is the location of the pressure sensor.

Fung and Yang [9] proposed a PI controller for the secondary fuel injection $\dot{m}_{\rm in}$, which, due to the differentiation in (7), gives a PD control law

$$u_{\rm in}(t)=-[K_P y(t-\tau_c)+K_D\dot{y}(t-\tau_c)] \tag{14}$$

where $\tau_c$ is the delay due to measurement, computation and actuation in the implementation of control. Substituting (14) into (12) we get

$$\begin{aligned}\ddot{\eta}_n+\omega_n^2\eta_n&+\sum_{i=1}^{\infty}(D_{ni}\dot{\eta}_i+E_{ni}\eta_i)\\&+\sum_{i=1}^{\infty}\sum_{j=1}^{\infty}(A_{nij}\dot{\eta}_i\dot{\eta}_j+B_{nij}\eta_i\eta_j)\\&+\frac{\bar{a}^2}{E_n^2}\sum_{k=1}^{M}\sum_{i=1}^{\infty}b(\mathbf{r}_k)\psi_n(\mathbf{r}_k)\psi_i(\mathbf{r}_s)[K_D\dot{\eta}_i(t-\tau_k)\\&+K_P\eta_i(t-\tau_k)]=0\end{aligned} \tag{15}$$

where $\tau_k=\tau(\mathbf{r}_k)+\tau_c$. Fung and Yang [9] showed that, *when all the parameters of the system are known*, (at least) the two-mode truncation of the system (15) can be stabilized by properly choosing $K_P$ and $K_D$. The next section shows how to tune $K_P$ and $K_D$ on-line when the parameters of the system are unknown.

## III. Adaptive Controller for the Average Two-Mode Model

In this paper we develop an adaptation technique for the PI controller (14). We replace the constant gains $K_D$ and $K_P$ by estimates $\hat{K}_D$ and $\hat{K}_P$

$$u_{\rm in}(t)=-[\hat{K}_P(t-\tau_c)y(t-\tau_c)+\hat{K}_D(t-\tau_c)\dot{y}(t-\tau_c)]. \tag{16}$$

In (15) this modification is accommodated by replacing $K_D$ and $K_P$ by $\hat{K}_D(t-\tau_k)$ and $\hat{K}_P(t-\tau_k)$, respectively.

Under the assumption that $\hat{K}_D$ and $\hat{K}_P$ are updated slowly, time averaging (see Nayfeh [19] for this particular application) of the model (15) gives equations for the modes in terms of their amplitudes $r_n$ and phases $\phi_n$. The two mode model given in Fung and Yang [9] is

$$\dot{r}_1=\alpha_{c1}r_1-\beta r_1r_2\cos\Phi \tag{17}$$

$$\dot{r}_2=\alpha_{c2}r_2+\beta r_1^2\cos\Phi \tag{18}$$

$$\dot{\Phi}=2\theta_{c1}-\theta_{c2}-\beta\left(\frac{r_1^2}{r_2}-2r_2\right)\sin\Phi \tag{19}$$

where $\Phi$ is the phase difference between the modes, defined as $\Phi=2\phi_1-\phi_2$. The constant $\beta$ is given by

$$\beta=\left(\frac{\bar{\gamma}+1}{8\bar{\gamma}}\right)\omega_1$$

and $\alpha_{cn}$ and $\theta_{cn}$, the closed-loop growth coefficients, are given by the expressions

$$\begin{aligned}\alpha_{cn}=\alpha_n-\frac{1}{2}\sum_{k=1}^{M}\Bigg[&\hat{K}_D(t-\tau_k)U_{nk}\cos(\omega_n\tau_k)\\&-\frac{\hat{K}_P(t-\tau_k)}{\omega_n}U_{nk}\sin(\omega_n\tau_k)\Bigg]\end{aligned} \tag{20}$$

$$\begin{aligned}\theta_{cn}=\theta_n+\frac{1}{2}\sum_{k=1}^{M}\Bigg[&\hat{K}_D(t-\tau_k)U_{nk}\sin(\omega_n\tau_k)\\&+\frac{\hat{K}_P(t-\tau_k)}{\omega_n}U_{nk}\cos(\omega_n\tau_k)\Bigg].\end{aligned} \tag{21}$$

The quantity $U_{nk}$ is the spatial distribution of the control input which is modeled as a set of $M$ point actuators, $\tau_k$ is the total time delay for the control input at each point, and $\omega_n$ is the frequency of each mode. We point out that in (19) we have corrected a sign error that appears in Fung and Yang [9].

When the coefficients $\alpha_1$ and $\alpha_2$ are known, the gains $\hat{K}_P$ and $\hat{K}_D$ can be selected fixed to achieve desired values of damping coefficients $\alpha_{c1}$ and $\alpha_{c2}$. When $\alpha_1$ and $\alpha_2$ are unknown or vary with operating conditions, $\hat{K}_P$ and $\hat{K}_D$ are continuously updated with the objective of driving $r_1$ and $r_2$ to zero. In order to derive the update laws for $\hat{K}_D$ and $\hat{K}_P$, in this section we assume that they enter (20) and (21) with $\tau_k=0$. The stability of the system with the delays included will be proved in Section V.

Combining (17)–(19) with (20) and (21), the equations for the closed-loop adaptive system are represented as

$$\dot{r}_1=\alpha_1r_1+(\gamma_1\hat{K}_D+\delta_1\hat{K}_P)r_1-\beta r_1r_2\cos\Phi \tag{22}$$

$$\dot{r}_2=\alpha_2r_2+(\gamma_2\hat{K}_D+\delta_2\hat{K}_P)r_2+\beta r_1^2\cos\Phi \tag{23}$$

$$\begin{aligned}\dot{\Phi}=2\theta_1-\theta_2+(2\omega_1\delta_1-\omega_2\delta_2)\hat{K}_D-\left(\frac{2\gamma_1}{\omega_1}-\frac{\gamma_2}{\omega_2}\right)\hat{K}_P\\-\beta\left(\frac{r_1^2}{r_2}-2r_2\right)\sin\Phi.\end{aligned} \tag{24}$$

The quantities $\gamma_1$, $\gamma_2$, $\delta_1$, and $\delta_2$ correspond to the terms multiplying $\hat{K}_D$ and $\hat{K}_P$ in (20) and (21).

Our design of a tuning mechanism for $\hat{K}_P$ and $\hat{K}_D$ is based on a Lyapunov function

$$V = \frac{1}{2}\left(r_1^2 + r_2^2 + \frac{1}{g_D}\tilde{K}_D^2 + \frac{1}{g_P}\tilde{K}_P^2\right) \tag{25}$$

where $\tilde{K}_D$ and $\tilde{K}_P$ are parameter estimation errors

$$\begin{aligned}\tilde{K}_D &= K_D - \hat{K}_D\\ \tilde{K}_P &= K_P - \hat{K}_P\end{aligned}$$

with constants $K_D$ and $K_P$ yet to be defined. The weighting coefficients $g_D, g_P > 0$ are referred to as the adaptation gains. The control objective is to drive $r_1$ and $r_2$ to zero, while keeping the errors $\tilde{K}_D$ and $\tilde{K}_P$ bounded. Taking the time derivative of $V$, we get

$$\begin{aligned}\dot{V} &= (\alpha_1 + \gamma_1\hat{K}_D + \delta_1\hat{K}_P)r_1^2 + (\alpha_2 + \gamma_2\hat{K}_D + \delta_2\hat{K}_P)r_2^2\\ &\quad - \frac{1}{g_D}\dot{\hat{K}}_D\tilde{K}_D - \frac{1}{g_P}\dot{\hat{K}}_P\tilde{K}_P\\ &= (\alpha_1 + \gamma_1 K_D + \delta_1 K_P)r_1^2 + (\alpha_2 + \gamma_2 K_D + \delta_2 K_P)r_2^2\\ &\quad - \left(\frac{1}{g_D}\dot{\hat{K}}_D + \gamma_1 r_1^2 + \gamma_2 r_2^2\right)\tilde{K}_D\\ &\quad - \left(\frac{1}{g_P}\dot{\hat{K}}_P + \delta_1 r_1^2 + \delta_2 r_2^2\right)\tilde{K}_P.\end{aligned} \tag{26}$$

To cancel the cross-terms generated by the parameter estimation errors $\tilde{K}_D$ and $\tilde{K}_P$, we select the update laws

$$\dot{\hat{K}}_D = -g_D\left(\gamma_1 r_1^2 + \gamma_2 r_2^2\right) \tag{27}$$

$$\dot{\hat{K}}_P = -g_P\left(\delta_1 r_1^2 + \delta_2 r_2^2\right). \tag{28}$$

Then $\dot{V}$ becomes

$$\dot{V} = (\alpha_1 + \gamma_1 K_D + \delta_1 K_P)r_1^2 + (\alpha_2 + \gamma_2 K_D + \delta_2 K_P)r_2^2. \tag{29}$$

To guarantee (global) stability of the equilibrium $r_1 = r_2 = \tilde{K}_P = \tilde{K}_D$ and the regulation of $r_1$ and $r_2$ to zero, we wish to have

$$\alpha_1 + \gamma_1 K_D + \delta_1 K_P < 0 \tag{30}$$

$$\alpha_2 + \gamma_2 K_D + \delta_2 K_P < 0. \tag{31}$$

The constants $K_P$ and $K_D$, which have thus far remained undefined, can always be selected to satisfy (30) and (31) provided

$$\gamma_1\delta_2 - \gamma_2\delta_1 \neq 0. \tag{32}$$

This condition amounts to a linear controllability condition with a PD controller. When this condition is not satisfied, it is possible that the PD controller (both the constant one and the self-tuning one) could increase the damping of one mode (for instance, a mode that is open-loop unstable) while decreasing the damping of the other mode or making it even unstable. When the "controllability" condition (32) is satisfied, the self-tuning controller will guarantee that $r_1$ and $r_2$ go to zero, *while a designer without exact knowledge of $\alpha_1$ and $\alpha_2$ would not be able to select constant $K_P$ and $K_D$ to satisfy* (30) *and* (31).

A fine point worth noting is that our analysis does not answer whether the "closed-loop damping coefficients" $\alpha_{c1}(t) = \alpha_1 + \gamma_1\hat{K}_D(t) + \delta_1\hat{K}_P(t)$ and $\alpha_{c2}(t) = \alpha_2 + \gamma_2\hat{K}_D(t) + \delta_2\hat{K}_P(t)$ converge to negative values or not. Indeed, all that we have set as an objective and achieved is that $r_1(t)$ and $r_2(t)$ go to zero. Following the results on invariant manifolds of adaptive nonlinear systems [15], it is possible that from a set of initial conditions of measure zero (that is, with zero probability), $\alpha_{c1}(t)$ and $\alpha_{c2}(t)$ converge to positive values. This, however, will not prevent $r_1(t)$ and $r_2(t)$ from going to zero, as the Lyapunov analysis shows.

As it can be seen in (27) and (28), the implementation of the update laws requires the knowledge of the parameters $\gamma_1$, $\gamma_2$, $\delta_1$, and $\delta_2$ in (22)–(24), which is a major modeling requirement. In Section VII we present a *nonlinear identification* procedure for determining these parameters from steady-state limit cycle data.

## IV. Simulations for the Average Model

To illustrate the self-tuning controller, we carried out simulations for the uncontrolled and controlled two mode models. These simulations are for the model (22)–(24) with the update laws (27) and (28).

The values of the parameters in these simulations were chosen as given by Fung and Yang [9]. The conditions for the existence of stable limit cycles in open loop are

$$\alpha_1\alpha_2 < 0 \tag{33}$$

$$2\alpha_1 + \alpha_2 < 0. \tag{34}$$

The equilibrium is given by

$$r_{10} = \frac{1}{\beta\cos\Phi_0}\sqrt{-\alpha_1\alpha_2} \tag{35}$$

$$r_{20} = \frac{1}{\beta\cos\Phi_0}\alpha_1 \tag{36}$$

$$\Phi_0 = \tan^{-1}\left[\frac{2\theta_1 - \theta_2}{2\alpha_1 + \alpha_2}\right]. \tag{37}$$

The values of the parameters $\alpha_1$, $\alpha_2$, $\theta_1$, and $\theta_2$ are taken as 0.0144, −0.0559, 0.0062, and 0.0178, respectively [9]. The value of the specific heat ratio $\bar{\gamma}$ is taken as 1.2 as in [9].

Open-loop simulations. Fig. 2 shows the equilibrium (35)–(37) in the $r_1$-$r_2$ plane for three different initial conditions and the phase variation with time.

Simulations with control. To prepare for the closed-loop simulations, we first calculate the constants $\gamma_1$, $\gamma_2$, $\delta_1$, and $\delta_2$ from the data in [9]. This calculation is explained in Appendix A. As shown in Fig. 3, our adaptive controller drives the oscillation amplitudes to zero ($r_2$ versus $r_1$ plot), although the phase need not necessarily converge to a constant. Fig. 4 shows the variation of $\hat{K}_D$ and $\hat{K}_P$ with time. The values of $\hat{K}_D$ and $\hat{K}_P$ increase from zero to some values which are optimal for the particular initial conditions on the amplitudes.

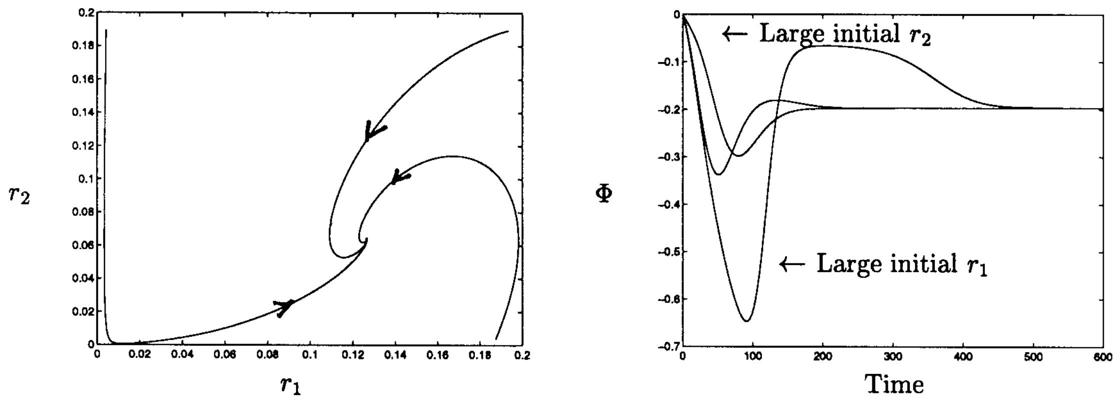


Fig. 2. Uncontrolled system.

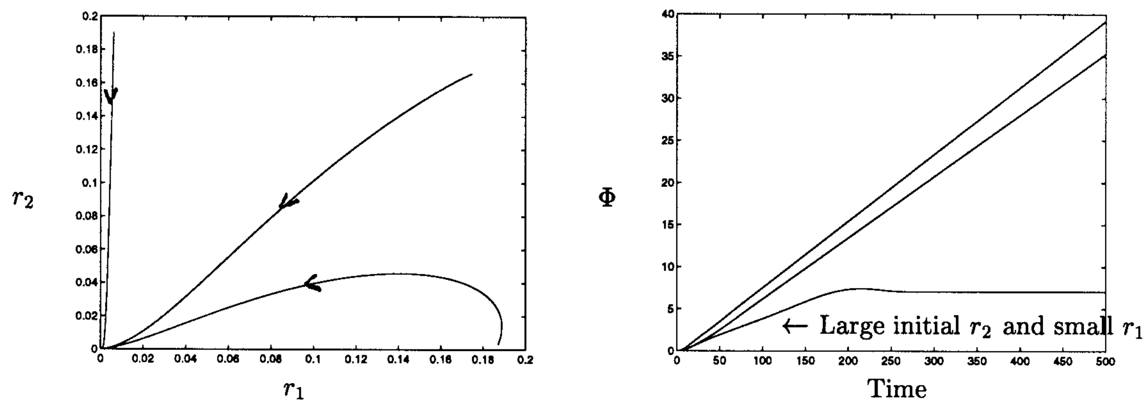


Fig. 3. Controlled system.

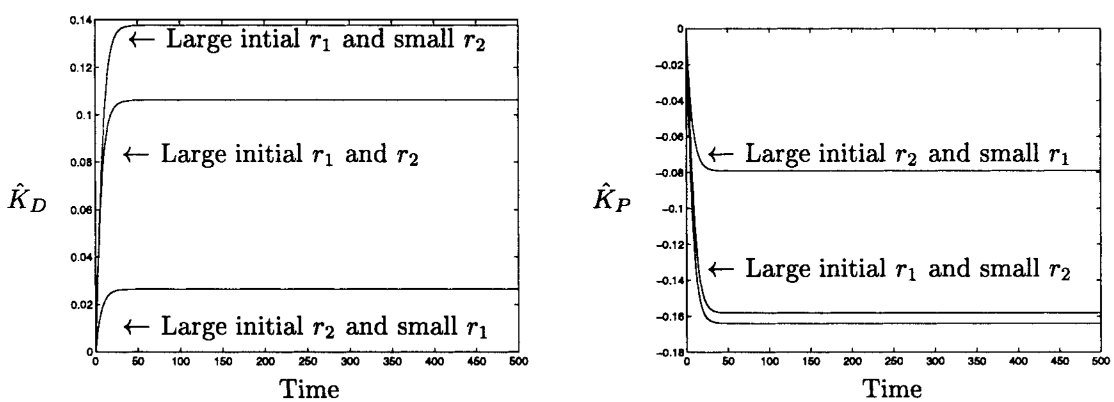


Fig. 4. Controlled system, $\hat{K}_D$ and $\hat{K}_P$ versus time.

## V. Robustness to Delay in Parameter Estimates

While the adaptation law in Section III were derived by assuming that $\hat{K}_D$ and $\hat{K}_P$ enter the system *without* the time delays $\tau_k$, in this section we ensure that stability is preserved in the presence of the delays. We consider the closed-loop system

$$\dot{r}_1(t) = \alpha_1 r_1(t) + \sum_{k=1}^{M}[\gamma_{1k}\hat{K}_D(t-\tau_k) + \delta_{1k}\hat{K}_P(t-\tau_k)]r_1(t) - \beta r_1(t) r_2(t)\cos\Phi(t) \tag{38}$$

$$\dot{r}_2(t) = \alpha_2 r_2(t) + \sum_{k=1}^{M}[\gamma_{2k}\hat{K}_D(t-\tau_k) + \delta_{2k}\hat{K}_P(t-\tau_k)]r_2(t) + \beta r_1^2(t)\cos\Phi(t) \tag{39}$$

$$\begin{aligned}\dot{\Phi}(t) = {} & 2\theta_1 - \theta_2 + \sum_{k=1}^{M}[(2\omega_1\delta_{1k} - \omega_2\delta_{2k})\hat{K}_D(t-\tau_k)] \\ & - \sum_{k=1}^{M}\left[\left(\frac{2\gamma_{1k}}{\omega_1} - \frac{\gamma_{2k}}{\omega_2}\right)\hat{K}_P(t-\tau_k)\right] \\ & - \beta\left(\frac{r_1^2(t)}{r_2(t)} - 2r_2(t)\right)\sin\Phi(t).\end{aligned} \tag{40}$$

where

$$\gamma_{nk} = -\frac{1}{2}U_{nk}\cos(\omega_n\tau_k) \tag{41}$$

$$\delta_{nk} = \frac{1}{2\omega_n}U_{nk}\sin(\omega_n\tau_k). \tag{42}$$

Assuming that "controllability condition" (32) holds, we select $K_D$ and $K_P$ such that

$$c_1 = -(\alpha_1 + \gamma_1 K_D + \delta_1 K_P) > 0 \tag{43}$$

$$c_2 = -(\alpha_2 + \gamma_2 K_D + \delta_2 K_P) > 0. \tag{44}$$

Now, let us take a Lyapunov function

$$U = \frac{1}{2}\left[r_1^2(t) + r_2^2(t) + \frac{1}{Mg_D}\sum_{k=1}^{M}\tilde{K}_D^2(t-\tau_k) + \frac{1}{Mg_P}\sum_{k=1}^{M}\tilde{K}_P^2(t-\tau_k)\right] + \rho_1\Omega_1 + \rho_2\Omega_2 \tag{45}$$

where $\rho_1$ and $\rho_2$ are positive constants yet to be determined, and

$$\Omega_1 = \frac{1}{M}\sum_{k=1}^{M}\left[\int_{t-\tau_k}^{t} r_1^2(s)\,ds\right] \tag{46}$$

$$\Omega_2 = \frac{1}{M}\sum_{k=1}^{M}\left[\int_{t-\tau_k}^{t} r_2^2(s)\,ds\right]. \tag{47}$$

Note that for $\tau_k \equiv 0$, the Lyapunov function $U$ reduces to the Lyapunov function $V$ in (25). Then we have

$$\begin{aligned}\dot{U} = &-\left(c_1 - \rho_1 + \sum_{k=1}^{M}[\gamma_{1k}\tilde{K}_D(t-\tau_k) + \delta_{1k}\tilde{K}_P(t-\tau_k)]\right)\\ &\times r_1^2(t) - \frac{1}{M}\sum_{k=1}^{M}[\rho_1 - \gamma_1\tilde{K}_D(t-\tau_k) - \delta_1\tilde{K}_P(t-\tau_k)]\\ &\times r_1^2(t-\tau_k) - \left(c_2 - \rho_2 + \sum_{k=1}^{M}[\gamma_{2k}\tilde{K}_D(t-\tau_k)\right.\\ &\left.+ \delta_{2k}\tilde{K}_P(t-\tau_k)]\right)r_2^2(t) - \frac{1}{M}\sum_{k=1}^{M}[\rho_2 - \gamma_2\tilde{K}_D\\ &\times (t-\tau_k) - \delta_2\tilde{K}_P(t-\tau_k)]r_2^2(t-\tau_k).\end{aligned} \tag{48}$$

Let us denote $\tilde{K} = [\tilde{K}_D \;\; \tilde{K}_P]^T$ and

$$\xi_1 = M\sqrt{\left(\max_k \gamma_{1k}\right)^2 + \left(\max_k \delta_{1k}\right)^2} \tag{49}$$

$$\xi_2 = M\sqrt{\left(\max_k \gamma_{2k}\right)^2 + \left(\max_k \delta_{2k}\right)^2}. \tag{50}$$

Then (48) yields

$$\begin{aligned}\dot{U} \le &-\left(c_1 - \rho_1 - \frac{\xi_1}{M}\sum_{k=1}^{M}|\tilde{K}(t-\tau_k)|\right)r_1^2(t)\\ &- \frac{1}{M}\sum_{k=1}^{M}(\rho_1 - \xi_1|\tilde{K}(t-\tau_k)|)r_1^2(t-\tau_k)\\ &- \left(c_2 - \rho_2 - \frac{\xi_2}{M}\sum_{k=1}^{M}|\tilde{K}(t-\tau_k)|\right)r_2^2(t)\\ &- \frac{1}{M}\sum_{k=1}^{M}(\rho_2 - \xi_2|\tilde{K}(t-\tau_k)|)r_2^2(t-\tau_k)\end{aligned} \tag{51}$$

where $|\tilde{K}|$ denotes the 2-norm of $\tilde{K}$. We see that if

$$|\tilde{K}_k(t-\tau_k)| < \frac{\rho_1}{\xi_1} < \frac{c_1}{2\xi_1} \tag{52}$$

$$|\tilde{K}_k(t-\tau_k)| < \frac{\rho_2}{\xi_2} < \frac{c_2}{2\xi_2} \tag{53}$$

for all $k = 1, \cdots, M$, then $\dot{U}(t) \le 0$. Denoting $g = \max\{g_D, g_P\}$, we see that

$$\begin{aligned}U(t) &\ge \frac{1}{2gM}\sum_{k=1}^{M}|\tilde{K}(t-\tau_k)|^2\\ &\ge \frac{1}{2gM}\max_k|\tilde{K}(t-\tau_k)|^2.\end{aligned} \tag{54}$$

Then, if we select

$$\rho_1 = \frac{c_1}{4} \tag{55}$$

$$\rho_2 = \frac{c_2}{4} \tag{56}$$

the set

$$U(0) < \frac{1}{32gM}\left(\min\left\{\frac{c_1}{\xi_1}, \frac{c_2}{\xi_2}\right\}\right)^2 \tag{57}$$

is positively invariant. This is easy to see because (57) along with (57) implies (52), (53), which, due to (55), (56), means that in the set (57) we have

$$\dot{U} \le -\frac{c_1}{2}r_1^2(t) - \frac{c_2}{2}r_2^2(t). \tag{58}$$

In addition, (58) proves that the equilibrium $r_1 = r_2 = \tilde{K}_D = \tilde{K}_P = 0$ is stable, and that the set (57) also belongs to its region of attraction. Finally, by LaSalle's theorem, (58) guarantees that $r_1(t)$ and $r_2(t)$ converge to zero.

It is important to properly interpret the regional result we have just established. From (45) and (57) it is clear that we are restricting the initial conditions on the estimation errors $\tilde{K}_D$ and $\tilde{K}_P$ to be sufficiently small. Since $\tilde{K}_D = K_D - \hat{K}_D$ and $\tilde{K}_P = K_P - \hat{K}_P$, where $K_D$ and $K_P$ are constants selected in our analysis to satisfy (43) and (44), it follows that we need initial conditions on the estimates $\hat{K}_D$ and $\hat{K}_P$ to be close to *some* of many possible *stabilizing* values of $K_D$ and $K_P$. *If we select the initial gains $\hat{K}_D$ and $\hat{K}_P$ to be zero*, then from (45) and (57) we require that there exist *some* $K_D$ and $K_P$ that satisfy (43), (44), and

$$\frac{1}{g_D}K_D^2 + \frac{1}{g_P}K_P^2 < \frac{1}{16gM}\left(\min\left\{\frac{c_1}{\xi_1}, \frac{c_2}{\xi_2}\right\}\right)^2. \tag{59}$$

We stress that the robustness result established in this section is achieved without any tools for update law robustification (leakage, projection, etc.). As we shall see in Section VIII-B, these tools will become necessary in the presence of substantial actuator limitations.

## VI. Implementation of the Update Laws Using a Single Pressure Sensor

While the control law of Fung and Yang [9] involves only the pressure measurements from a single sensor, it may appear that a sophisticated scheme (with distributed sensors) would be necessary to measure the mode amplitudes $r_1$ and $r_2$ needed to implement the update laws (27) and (28). Fortunately, this is not the case and we can employ a single pressure sensor which in the average sense performs the same task of adaptation as the scheme which employs the mode amplitudes.

We now postulate, and later prove, that the update laws (27) and (28) can be replaced by the following expressions for $\hat{K}_D$ and $\hat{K}_D$:

$$\dot{\hat{K}}_D = -(a_1 y^2 + a_2 \dot{y}^2) \tag{60}$$

$$\dot{\hat{K}}_P = -(b_1 y^2 + b_2 \dot{y}^2). \tag{61}$$

In the following, we show that the constants $a_1$, $a_2$, $b_1$, and $b_2$ can be found such that the average equations of (60) and (61) are given by (27) and (28). Using (13)

$$y = \bar{p}\sum_{n=1}^{\infty}\eta_n\psi_n \approx \bar{p}(\eta_1\psi_1 + \eta_2\psi_2) \tag{62}$$

we get (60) and (61) in the form

$$\dot{\hat{K}}_D = -\bar{p}^2[a_1(\eta_1\psi_1 + \eta_2\psi_2)^2 + a_2(\dot{\eta}_1\psi_1 + \dot{\eta}_2\psi_2)^2] \tag{63}$$

$$\dot{\hat{K}}_P = -\bar{p}^2[b_1(\eta_1\psi_1 + \eta_2\psi_2)^2 + b_2(\dot{\eta}_1\psi_1 + \dot{\eta}_2\psi_2)^2] \tag{64}$$

where $\psi_1$ and $\psi_2$ represent the values of the mode functions at the point of measurement. Substituting the mode $\eta_n$ by

$$\eta_n = r_n \sin(\omega_n t + \phi_n) \tag{65}$$

and its derivative by its approximation

$$\dot{\eta}_n \approx r_n\omega_n \cos(\omega_n t + \phi_n), \tag{66}$$

after averaging we get

$$\dot{\hat{K}}_D = -\frac{\bar{p}}{2}\left[\left(a_1 + \omega_1^2 a_2\right)\psi_1^2 r_1^2 + \left(a_1 + \omega_2^2 a_2\right)\psi_2^2 r_2^2\right] \tag{67}$$

$$\dot{\hat{K}}_P = -\frac{\bar{p}}{2}\left[\left(b_1 + \omega_1^2 b_2\right)\psi_1^2 r_1^2 + \left(b_1 + \omega_2^2 b_2\right)\psi_2^2 r_2^2\right]. \tag{68}$$

Comparing these equations to the expressions (27) and (28) we solve for $a_1$, $a_2$, $b_1$, and $b_2$

$$a_1 = \frac{2g_D}{\bar{p}^2\left(\omega_2^2 - \omega_1^2\right)}\left(\frac{\gamma_1\omega_2^2}{\psi_1^2} - \frac{\gamma_2\omega_1^2}{\psi_2^2}\right) \tag{69}$$

$$a_2 = \frac{2g_D}{\bar{p}^2\left(\omega_1^2 - \omega_2^2\right)}\left(\frac{\gamma_1}{\psi_1^2} - \frac{\gamma_2}{\psi_2^2}\right) \tag{70}$$

$$b_1 = \frac{2g_P}{\bar{p}^2\left(\omega_2^2 - \omega_1^2\right)}\left(\frac{\delta_1\omega_2^2}{\psi_1^2} - \frac{\delta_2\omega_1^2}{\psi_2^2}\right) \tag{71}$$

$$b_2 = \frac{2g_P}{\bar{p}^2\left(\omega_1^2 - \omega_2^2\right)}\left(\frac{\delta_1}{\psi_1^2} - \frac{\delta_2}{\psi_2^2}\right). \tag{72}$$

The coefficient $\bar{p}$ can be eliminated by replacing $g_D$ and $g_P$ in the Lyapunov function (25) by $g_D/\bar{p}^2$ and $g_P/\bar{p}^2$, respectively. Thus, in order to implement the update laws (60), (61), we need only the knowledge of the mode shapes, mode frequencies, and the constants $\gamma_1$, $\gamma_2$, $\delta_1$, and $\delta_2$, which we estimate in the next section.

*Remark 6.1:* Even though high pressure sensors are available, and one can obtain clean measurements of pressure which allow the calculation of $\dot{y}$, in some situations it may be desirable to avoid using the derivative of pressure. Such situations are easy to accommodate by replacing the derivative of pressure by its integral in (60) and (61)

$$\dot{\hat{K}}_D = -(a_1 y^2 + a_2 z^2) \tag{73}$$

$$\dot{\hat{K}}_P = -(b_1 y^2 + b_2 z^2). \tag{74}$$

where $z(t) = \int_0^t y(\sigma)\,d\sigma$. In this case the coefficients (69)–(72) would be defined by

$$a_1 = \frac{2g_D}{\bar{p}^2\left(\omega_1^2 - \omega_2^2\right)}\left(\frac{\gamma_1\omega_1^2}{\psi_1^2} - \frac{\gamma_2\omega_2^2}{\psi_2^2}\right) \tag{75}$$

$$a_2 = \frac{2g_D\omega_1^2\omega_2^2}{\bar{p}^2\left(\omega_2^2 - \omega_1^2\right)}\left(\frac{\gamma_1}{\psi_1^2} - \frac{\gamma_2}{\psi_2^2}\right) \tag{76}$$

$$b_1 = \frac{2g_P}{\bar{p}^2\left(\omega_1^2 - \omega_2^2\right)}\left(\frac{\delta_1\omega_1^2}{\psi_1^2} - \frac{\delta_2\omega_2^2}{\psi_2^2}\right) \tag{77}$$

$$b_2 = \frac{2g_P\omega_1^2\omega_2^2}{\bar{p}^2\left(\omega_2^2 - \omega_1^2\right)}\left(\frac{\delta_1}{\psi_1^2} - \frac{\delta_2}{\psi_2^2}\right). \tag{78}$$

## VII. Identification of the Constants $\gamma_1$, $\gamma_2$, $\delta_1$ and $\delta_2$

In this paper we are concerned with the problem of stabilization in the presence of a varying equivalence ratio, and assume that its variation affects only the open-loop growth coefficients $\alpha_1$ and $\alpha_2$ but not the control input coefficients $\gamma_1$, $\gamma_2$, $\delta_1$, and $\delta_2$. The coefficients $\gamma_1$, $\gamma_2$, $\delta_1$ and $\delta_2$ need to be known in order for the adaptation laws (27), (28), or (60), (61), and (69)–(72) to be implemented. These coefficients would be difficult to identify if the model were linear. Our approach to the problem via a nonlinear model allows us to identify those coefficients easily using only *steady-state* limit cycle data.

Consider an identification experiment with fixed values of $\hat{K}_D$ and $\hat{K}_P$, denoted simply as $K_D$ and $K_P$. The equilibrium equations for (22) and (23) have the form

$$\frac{\alpha_1}{\beta}+\frac{\gamma_1}{\beta}K_D+\frac{\delta_1}{\beta}K_P=r_2\cos\Phi \tag{79}$$

$$\frac{\alpha_2}{\beta}+\frac{\gamma_2}{\beta}K_D+\frac{\delta_2}{\beta}K_P=-\frac{r_1^2}{r_2}\cos\Phi. \tag{80}$$

We now outline a procedure for identifying $\gamma_1/\beta$, $\delta_1/\beta$, $\gamma_2/\beta$ and $\delta_2/\beta$. These quantities can be employed in (27), (28), or (69)–(72) instead of $\gamma_1$, $\gamma_2$, $\delta_1$, and $\delta_2$ by treating $\beta$ as a part of the adaptation gain.

Equations (79) and (80) have the linear form

$$A_1+B_1^TX=Y \tag{81}$$

$$A_2+B_2^TX=Z \tag{82}$$

where $A_k=\alpha_k/\beta$ and $B_k^T=[\gamma_k/\beta,\ \delta_k/\beta]$ for $k=1,2$, and

$$X=[K_D,K_P]^T \tag{83}$$

$$Y=r_2\cos\Phi \tag{84}$$

$$Z=-\frac{r_1^2}{r_2}\cos\Phi. \tag{85}$$

We can therefore use the least-squares linear regression to find the best estimate of $\gamma_1/\beta$, $\delta_1/\beta$, $\gamma_2/\beta$ and $\delta_2/\beta$ from a series of experiments in which we measure $r_1$, $r_2$, and $\Phi$. Let $X_i$, $Y_i$, and $Z_i$ denote the values of $X$, $Y$, and $Z$ in $N$ different experiments. Then the estimates

$$\begin{bmatrix}\gamma_1/\beta\\ \delta_1/\beta\end{bmatrix}=\left[\sum_{i=1}^N X_iX_i^T-\frac{\left(\sum_{j=1}^N X_j\right)\left(\sum_{i=1}^N X_i\right)^T}{N}\right]^{-1}\times\left[\sum_{i=1}^N X_iY_i-\frac{\left(\sum_{i=1}^N X_i\right)\left(\sum_{j=1}^N Y_j\right)}{N}\right] \tag{86}$$

$$\begin{bmatrix}\gamma_2/\beta\\ \delta_2/\beta\end{bmatrix}=\left[\sum_{i=1}^N X_iX_i^T-\frac{\left(\sum_{j=1}^N X_j\right)\left(\sum_{i=1}^N X_i\right)^T}{N}\right]^{-1}\times\left[\sum_{i=1}^N X_iZ_i-\frac{\left(\sum_{i=1}^N X_i\right)\left(\sum_{j=1}^N Z_j\right)}{N}\right] \tag{87}$$

are easily shown to be the minimizers of the cost functional

$$J=\sum_{i=1}^N\left(Y_i-A_1-B_1^TX_i\right)^2+\sum_{i=1}^N\left(Z_i-A_2-B_2^TX_i\right)^2 \tag{88}$$

with respect to $B_1$ and $B_2$.

Note that in the above procedure $\alpha_1$ and $\alpha_2$ are treated as unknown but constant. Once the identification of $\gamma_1/\beta$, $\delta_1/\beta$, $\gamma_2/\beta$ and $\delta_2/\beta$ is performed for a constant equivalence ratio, the adaptation laws (27), (28) can be used to adapt the PD controller to the actual $\alpha_1$ and $\alpha_2$ which vary with the equivalence ratio.

The key for implementing the procedure (83)–(88) is the availability of the amplitudes of the modes $r_1$ and $r_2$ and the phase shift $\Phi$. Computing these quantities ($\Phi$ in particular) from time traces of $p$ for a system in a limit cycle, turns out to be a nontrivial task. In Section VIII we explain how $r_1$, $r_2$, and $\Phi$ are calculated using an LMS algorithm.

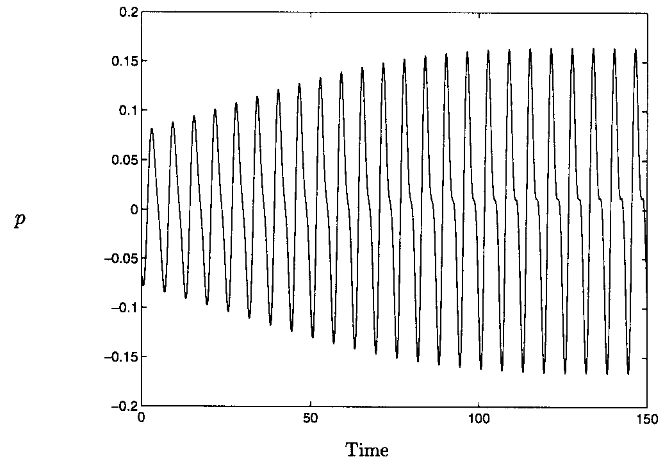


Fig. 5. Nonaverage system without control, pressure versus time.

## VIII. Simulation for Nonaverage Model

The update law using a single pressure sensor was implemented on the nonaverage two-mode model

$$\begin{aligned}&\ddot\eta_n-2\alpha_n\dot\eta_n+\left(\omega_n^2-2\omega_n\theta_n\right)\eta_n\\&\quad+\sum_{i=1}^2\sum_{j=1}^2[A_{nij}\dot\eta_i\dot\eta_j+B_{nij}\eta_i\eta_j]\\&\quad+\frac{\bar a^2}{E_n^2}\sum_{k=1}^M\sum_{i=1}^2[\hat K_D(t-\tau_k)\dot\eta_i(t-\tau_k)\\&\quad+\hat K_P(t-\tau_k)\eta_i(t-\tau_k)]b(\mathbf{r}_k)\psi_n(\mathbf{r}_k)\psi_i(\mathbf{r}_s)=0\end{aligned} \tag{89}$$

where $n=1,2$ and Numerical values of $\alpha_n$, $\theta_n$, and and $\bar\gamma$ are taken from [9] as in the averaged case. The expressions for $A_{nij}$ and $B_{nij}$ are taken from Culick [5] and are given as

$$\begin{aligned}A_{nij}=&\frac{I_{nij}}{4\bar\gamma\omega_i^2\omega_j^2}\left[\left(\omega_i^2+\omega_j^2\right)^2-\omega_n^4-4\bar\gamma\omega_i^2\omega_j^2\right]\\&+\frac{I_{nij}}{2\bar\gamma\omega_i^2\omega_j^2}\left(\omega_j^2-\omega_i^2\right)\left(\omega_j^2+\omega_i^2-\omega_n^2\right)\end{aligned} \tag{90}$$

$$B_{nij}=\frac{(\bar\gamma-1)I_{nij}}{2\bar\gamma}\left(\omega_j^2+\omega_i^2\right)+\frac{(\bar\gamma-1)I_{nij}}{2\bar\gamma}\left(\omega_j^2-\omega_i^2\right) \tag{91}$$

where

$$I_{nij}=\int\psi_n\psi_i\psi_j\,dV. \tag{92}$$

With the assumption that oscillations are purely longitudinal in a uniform chamber, the mode functions $\psi_n$ are given as $\psi_n=\cos\frac{n\pi z}{L}$.

Open-loop simulations of the system show a limit cycle as in the averaged case. The time trace of the pressure for this model, as sensed at one end of the chamber, is given in Fig. 5.

### A. Closed-Loop Simulations Without Actuator Limits

The simulations are carried out with the assumption that the distribution of the control input is uniform in space, i.e., $b_k=1$ for all $M$ points in the discrete approximation. The

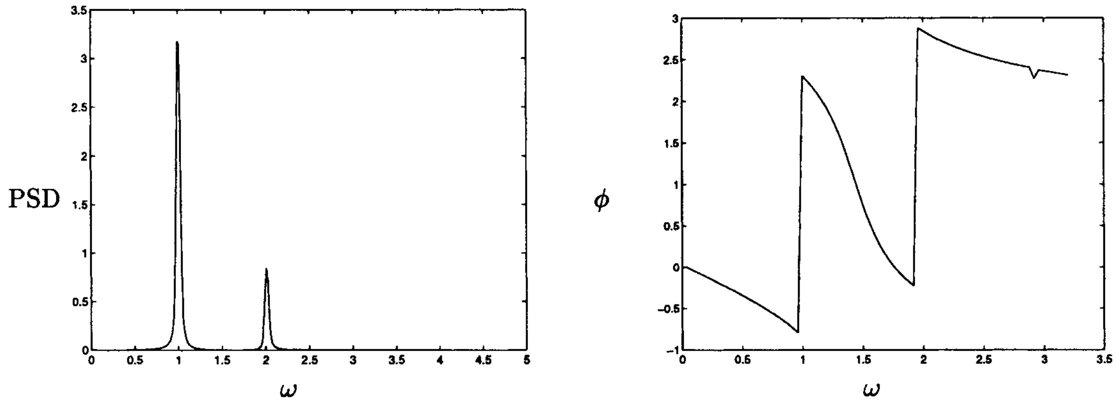


Fig. 6. The power spectral density and the phase of the Fourier transform of the pressure in the nonaverage uncontrolled system.

pressure sensor is assumed to be at one end of the chamber where $\psi_n(\mathbf{r}_s) = 1$. $\psi_i(\mathbf{r}_k)$ is taken as unity assuming that the length over which the secondary fuel burns is small. Secondary fuel combustion is approximated by four point actuators, i.e., $M = 4$ and the time delay is taken as one fourth of the time period of the first mode. The delayed values of

$$u_{\text{in}}(t) = \hat{K}_D(t-\tau_c)\dot{y}(t-\tau_c) + \hat{K}_P(t-\tau_c)y(t-\tau_c) \tag{93}$$

are needed to obtain $U_n(t)$. This is implemented using the second-order Padé approximation of a pure time delay (it is not clear why the pure delay would be a better description of the heat release process anyway), which, for a time delay $T$, is given by

$$G(s) = \frac{s^2T^2 - 4sT + 8}{s^2T^2 + 4sT + 8}. \tag{94}$$

The system parameters $\gamma_1$, $\gamma_2$, $\delta_1$ and $\delta_2$ are identified using the procedure described in Section VII. The system was simulated with various small destabilizing values of $K_D$ and $K_P$. The (79) and (80) require accurate values of $r_1$, $r_2$, and $\cos(\Phi)$. These three quantities are found using the pressure signal as follows. The phase $\phi$ of the pressure signal, observed by Fourier analysis using MATLAB and shown in Fig. 6, has sharp jumps at the two modal frequencies. Hence the value of $\cos(\Phi)$ obtained from the Fourier transform is not sufficiently accurate. Instead, we use an LMS based identification procedure to identify $r_1$, $r_2$, and $\Phi$. The pressure signal is assumed to be of the form

$$p = r_1 \sin(\omega_1 t + \phi_1) + r_2 \sin(\omega_2 t + \phi_2) \tag{95}$$

which can be represented linearly as

$$p = X^T W \tag{96}$$

where the "parameter" vector is

$$W = [r_1\cos(\phi_1) \quad r_1\sin(\phi_1) \quad r_2\cos(\phi_2) \quad r_2\sin(\phi_2)]^T \tag{97}$$

and the regressor vector is

$$X = [\sin(\omega_1 t) \quad \cos(\omega_1 t) \quad \sin(\omega_2 t) \quad \sin(\omega_2 t)]^T. \tag{98}$$

The estimation error, at any instant $k$, can be expressed as

$$e_k = p_k - X_k^T \hat{W}_k. \tag{99}$$

The parameter update law is

$$\hat{W}_{k+1} = \hat{W}_k + 2\mu e_k X_k. \tag{100}$$

Since we have four "parameters" in $W$, and two sinusoids with distinct frequencies in the regressor $X$, we have persistent excitation, and our estimates of $r_1$, $r_2$, and $\Phi$ converge to the true values. The constants $a_1$, $a_2$, $b_1$, and $b_2$ needed in (60) and (61) are determined from the (69)–(72). The destabilizing values of $K_D$ and $K_P$ used for identification should be small when compared to the critical values for the existence of limit cycles as obtained from (33) and (34). The resulting pressure signal in this case is closer to the sum of two sinusoids and hence the measure of the phase between them is more accurate when the LMS method is used.

The closed-loop simulations show that the controller drives the oscillation amplitudes to zero. The time traces of the pressure and the control input to the system are given in Fig. 7. Fig. 8 shows the variation in $\hat{K}_D$ and $\hat{K}_P$ with time. The values of $\hat{K}_D$ and $\hat{K}_P$ increase from zero to stabilizing values which reduce oscillation amplitudes to zero.

### *B. Simulations with Magnitude and Rate Saturations*

Simulations were also carried out to observe the effects of actuator limits on the system. While implementing the saturation of $u_{\text{in}} \propto \frac{d}{dt}\dot{m}_{\text{in}}$ (rate saturation) is simple, the saturation of $\dot{m}_{\text{in}}$ (magnitude saturation) requires more care. To saturate $\dot{m}_{\text{in}}$, the time derivative of $\dot{m}_{\text{in}}$ is set to zero when $|\dot{m}_{\text{in}}|$ exceeds the maximum and the derivative is in the direction of increase in this quantity.

The time trace of the pressure under magnitude and rate limit is given in Fig. 9. The limit cycles are observed to decrease but not go to zero. The uniformly rate limited decreasing trend of $\dot{m}_{\text{in}}$ in the first 20–30 s is arrested by the limit on $|\dot{m}_{\text{in}}|$ and the subsequent time trace shows large variations in $\dot{m}_{\text{in}}$. Fig. 10 shows the variation in $\hat{K}_D$ and $\hat{K}_P$ with time. These gains continue to increase since they are updated using the amplitudes of the modes which do not decrease to zero in this case. Even in the absence of magnitude

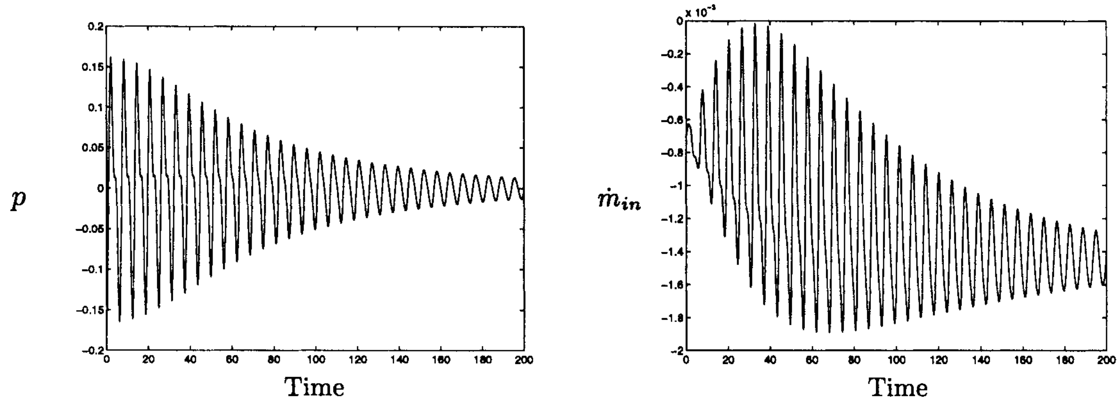


Fig. 7. Nonaverage system with control, pressure and $\dot{m}_{\rm in}$ versus time.

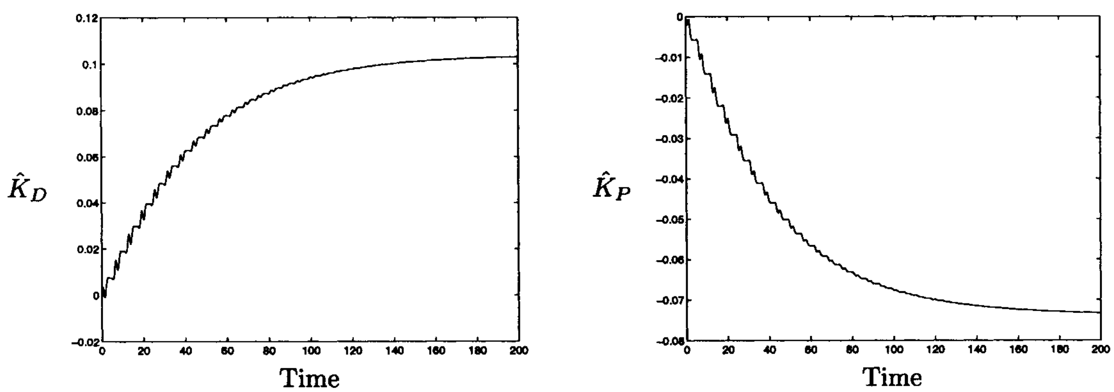


Fig. 8. Nonaverage system with control, $\hat{K}_D$ and $\hat{K}_P$ versus time.

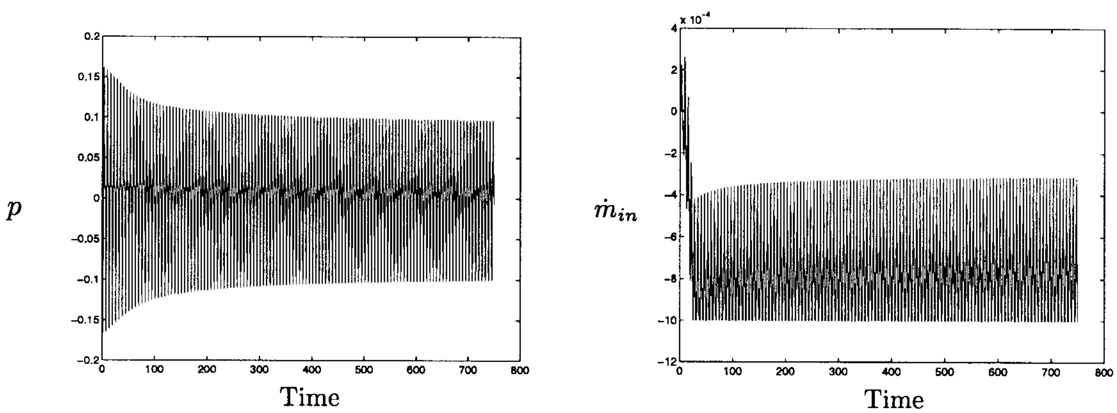


Fig. 9. Nonaverage system with control (magnitude and rate saturation)—pressure and $\dot{m}_{\rm in}$ versus time.

limits (when only the rate limit is present), the parameter drift occurs. We deal with the effects of parameter drift at the end of this section.

### *C. Robustification with Leakage*

It is observed in the previous cases with magnitude and/or rate saturation that the amplitudes of the modes do not go to zero. The parameter drift observed for $\hat{K}_D$ and $\hat{K}_P$ can be expected from the (27) and (28). We can prevent the parameter drift by using tools for robustification of the update law [14] such as fixed leakage, switching leakage, projection, etc. The latter two would require *a priori* knowledge of a set of stabilizing values of $K_D$ and $K_P$, and the estimates would usually converge to the boundary of the set, which means that the controller would end up being as conservative as a robust controller designed only on the basis of a priori information (and not on the basis of on-line information and learning the system). For this reason, we resort to fixed leakage, which is known to introduce a bias in regulation even in the absence of the nonparametric uncertainty that is causing the parameter

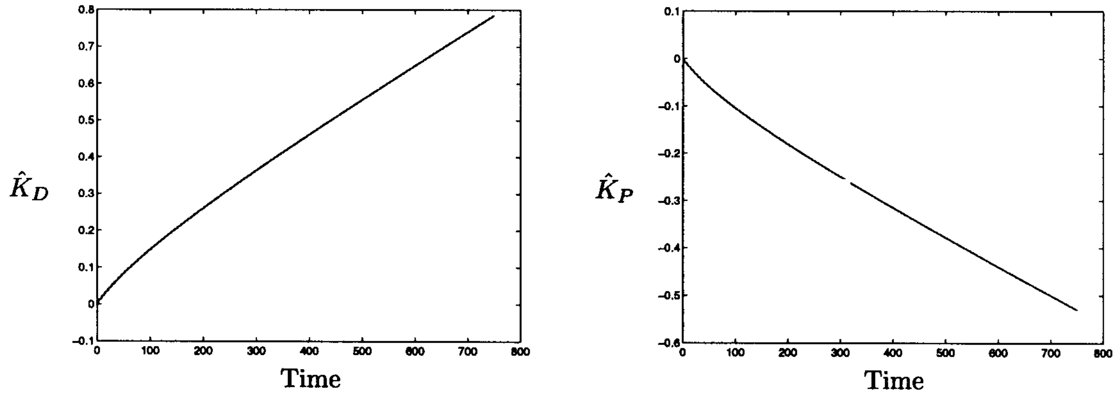


Fig. 10. Nonaverage system with control (magnitude and rate saturation)—$\hat{K}_D$ and $\hat{K}_P$ versus time.

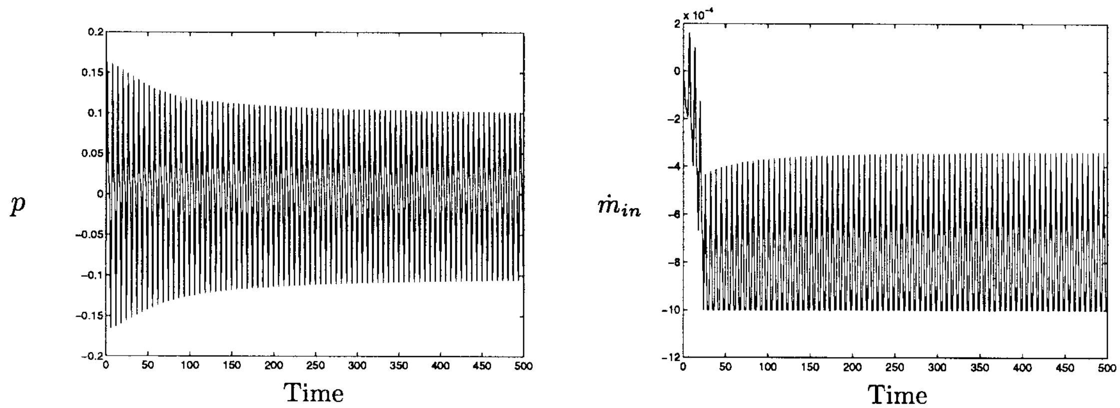


Fig. 11. Magnitude and rate saturation with leakage—pressure and $\dot{m}_{\rm in}$ versus time.

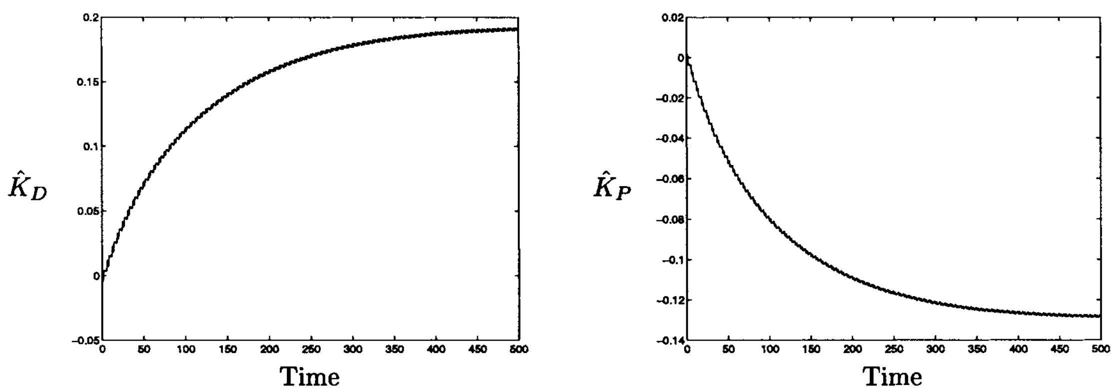


Fig. 12. Magnitude and rate saturation with leakage—$\hat{K}_D$ and $\hat{K}_P$ versus time.

drift. In the case of the model in this paper, the fixed leakage would result in a limit cycle even in the absence of actuator limitations. If small, we regard such a bias acceptable because, in the presence of actuator limitations, the feedback can only reduce the size of the limit cycle but cannot completely eliminate it. A leakage term is hence introduced in the update laws (60) and (61)

$$\dot{\hat{K}}_D = -(a_1 p^2 + a_2 \dot{p}^2) - \sigma_1 \hat{K}_D \tag{101}$$

$$\dot{\hat{K}}_P = -(b_1 p^2 + b_2 \dot{p}^2) - \sigma_2 \hat{K}_P \tag{102}$$

where $\sigma_1$ and $\sigma_2$ are positive constants. With rate saturation and magnitude saturation as in the previous subsection, a small leakage is found to affect the size of limit cycles minimally, see the pressure and $\dot{m}_{\rm in}$ plots in Fig. 11. As observed in Fig. 12, the gains $\hat{K}_D$ and $\hat{K}_P$ converge to values larger than in Fig. 8. The boundedness of signals (local) under leakage can be rigorously established using the same type of Lyapunov analysis (lengthy but straightforward) as in [14] and employing the Lyapunov function (25).

## IX. CONCLUSION

This paper presents an adaptive design and analysis of implementation issues for a two model Galerkin truncation of a nonlinear model of combustion instabilities. The following questions are beyond the scope of this paper and remain a subject for future work: 1) validation on higher order models and design of controllers of higher dynamic order for higher order models; 2) incorporation of a more detailed model of heat release into the control design; and 3) experimental verification.

## APPENDIX

Calculation of $\boldsymbol{\gamma_1}$, $\boldsymbol{\gamma_2}$, $\boldsymbol{\delta_1}$, and $\boldsymbol{\delta_2}$ from the data in [9]. The optimal values of $K_D$ and $K_P$ from [9] with an unstable first mode are 0.013 and $-0.0144$. The values, $\alpha_{c1} = 0.0053$ and $\alpha_{c2} = -0.0582$ are used in the expression for $\alpha_{cn}$ [(20)] to find $\gamma_1 = -0.3144$ and $\delta_1 = 0.3482$. Here, the secondary fuel is modeled as a 15-point actuator. The spatial distribution of the actuator power output $b_k$ is represented by a one-dimensional trapezoidal function. The total time delay of the fuel combustion process is taken as one-quarter of the time period of the fundamental mode $T_1$. Thus $\gamma_1$ is obtained by multiplying a quarter cosine wave with the distribution of $b_k$ [(20)]. Similarly, a quarter sine wave is multiplied with the $b_k$ distribution to give $\delta_1$. As $\omega_1 = 1$ and $\omega_2 = 2$, using (20), we have $\gamma_2$ nearly equal to zero as a trapezoidal distribution is multiplied by a cosine distribution from zero to $\pi$. Since some time delay is also associated with the computation process in the feedback the value of $\gamma_2$ is not chosen as zero but taken as $-0.1$. The value $\delta_1$ is approximately the summation over zero to $\frac{\pi}{2}$ of a sine multiplying a trapezoidal distribution between zero and $\frac{\pi}{2}$. The quantity $\delta_2$ would be the summation over zero to $\pi$ of a sine multiplying a trapezoidal distribution over zero and $\pi$. Therefore, the value of $\delta_2$ is chosen as 0.3 which is slightly less than the value of $\delta_1$.

## ACKNOWLEDGMENT

The authors thank K. Ariyur, J. McVey, R. Murray, A. Peracchio, B. Proscia, G. Ray, and T. Rosfjord for various forms of interaction on combustion instabilities.

## REFERENCES

[1] A. M. Annaswamy and A. F. Ghoniem, "Active control in combustion systems," *IEEE Contr. Syst. Mag.*, vol. 15, pp. 49–63.

[2] A. M. Annaswamy, J. P. Hathout, M. Fleifil, and A. F. Ghoniem, "Impact of linear coupling on the design of active controller for the thermoacoustic instability," submitted to *Combustion Sci. Technol.*, Oct. 1996.

[3] G. Billoud, M. A. Galland, C. Huynh Huu, and S. Candel, "Adaptive active control of combustion instabilities," *Combustion Sci. Technol.*, vol. 81, pp. 257–283, 1992.

[4] G. J. Bloxsidge, A. P. Dowling, N. Hooper, and P. J. Langhorne, "Active control of an acoustically driven combustion instability," *J. Theoretical Appl. Mechanics*, supplement to vol. 6, 1987.

[5] F. E. C. Culick, "Nonlinear behavior of acoustic waves in combustion chambers-I," *Acta Astronautica*, vol. 3, pp. 715–734, 1976.

[6] F. E. C. Culick, "Combustion instabilities in liquid-fueled propulsion systems—An overview," in *AGARD Conf. Proc.*, 1988, no. 40.

[7] M. Fleifil, A. M. Annaswamy, S. Ghoniem, and A. F. Ghoniem, "Active control of thermoacoustic instability in combustion systems," in *Proc. 4th IEEE Conf. Contr. Applicat.*, Albany, NY, Sept. 1995, pp. 685–690.

[8] M. Fleifil, A. M. Annaswamy, J. P. Hathout, and A. F. Ghoniem, "The origin of secondary peaks with active control of thermoacoustic instability," submitted to *Combustion Sci. Technol.*, Mar. 1997.

[9] Y.-T. Fung and V. Yang, "Active control of nonlinear pressure oscillations in combustion chambers," *J. Propulsion Power*, vol. 8, pp. 1282–1289, 1992.

[10] Y.-T. Fung, V. Yang, and A. Sinha, "Active control of combustion instabilities with distributed actuators," *Combustion Sci. Technol.*, vol. 78, pp. 217–245, 1991.

[11] A. Gulati and R. Mani, "Active control of unsteady combustion-induced oscillations," *J. Propulsion Power*, vol. 8, pp. 1109–1115, 1992.

[12] W. M. Haddad, A. Leonessa, J. R. Corrado, and V. Kapila, "State-space modeling and robust reduced-order control of combustion instabilities," in *Proc. 1997 Amer. Contr. Conf.*, pp. 3125–3129.

[13] J. P. Hathout, A. M. Annaswamy, M. Fleifil, and A. F. Ghoniem, "A model-based active control design for thermoacoustic instability," submitted to *Combustion Sci. Technol.*, May 1997.

[14] P. A. Ioannou and J. Sun, *Robust Adaptive Control*. Englewood Cliffs, NJ: Prentice-Hall, 1995.

[15] M. Krstić, "Invariant manifolds and asymptotic properties of adaptive nonlinear systems," *IEEE Trans. Automat. Contr.*, vol. 41, pp. 817–829, 1996.

[16] W. Lang, T. Poinsot, and S. Candel, "Active control of combustion instability," *Combustion and Flame*, vol. 7, pp. 281–289, 1987.

[17] P. J. Langhorne, A. P. Dowling, and N. Hooper, "Practical active control systems for combustion oscillations," *J. Propulsion Power*, vol. 6, pp. 324–333, 1990.

[18] K. R. McManus, U. Vandsburger, and C. T. Bowman, "Combustor performance enhancement through direct shear layer excitation," *Combustion and Flame*, vol. 82, pp. 75–92, 1990.

[19] A. H. Nayfeh, *Perturbation Methods*. New York: Wiley, 1973.

[20] Y. Neumeier and B. T. Zinn, "Active control of combustion instabilities using real time identification of unstable combustor modes," in *Proc. 4th IEEE Conf. Contr. Applicat.*, Albany, NY, Sept. 1995, pp. 691–698.

[21] L. G. Paparizos and F. E. C.Culick, "The two-mode approximation to nonlinear acoustics in combustion chambers 1: Exact solution for second-order acoustics," *Combustion Sci. Technol.*, vol. 65, pp. 39–65, 1989.

[22] T. Poinsot, F. Bourienne, S. Candel, and E. Esposito, "Suppression of combustion instabilities by active control," *J. Propulsion Power*, vol. 5, pp. 14–20, 1989.

[23] J. D. Sterling, "Nonlinear analysis and modeling of combustion instabilities in a laboratory combustor," *Combustion Sci. Technol.*, vol. 89, pp. 167–179, 1993.

[24] J. E. Tierno and J. C. Doyle, "Multimode active stabilization of a Rijke tube," in *DSC-Vol. 38, ASME Winter Annu. Meet.*, 1992.

[25] V. Yang, A. Sinha, and Y.-T. Fung, "State feedback control of longitudinal combustion instabilities," *J. Propulsion Power*, vol. 8, 1992.

**Miroslav Krstic** received the B.S.E.E. degree from the University of Belgrade, Yugoslavia, and the Ph.D. degree from the University of California, Santa Barbara, in 1994.

During 1995 to 1997 he was Assistant Professor of Mechanical Engineering at the University of Maryland. He is Associate Professor in the Department of Applied Mechanics and Engineering Sciences at the University of California at San Diego. He is a coauthor of the books *Nonlinear and Adaptive Control Design* (New York: Wiley, 1995) and *Stabilization of Nonlinear Uncertain Systems* (New York: Springer-Verlag, 1998). His research interests include nonlinear, adaptive, robust, and stochastic control theory for finite-dimensional and distributed parameter systems, and applications to propulsion systems and flows.

Dr. Kristic's dissertation received the UCSB Best Dissertation Award. He is a recipient of several paper awards, including the George S. Axelby Outstanding Paper Award of the IEEE TRANSACTIONS ON AUTOMATIC CONTROL and the O. Hugo Schuck Award for the best paper at American Control Conference. He has also received the National Science Foundation Career Award, Office of Naval Research Young Investigator Award, and the Presidential Early Career Award for Scientists and Engineers (PECASE). He serves as Associate Editor for the IEEE TRANSACTIONS ON AUTOMATIC CONTROL, *International Journal of Adaptive Control and Signal Processing*, and *Systems and Control Letters*.

**Ashish Krupadanam** was born in India in 1974. He received the B.Tech. degree in mechanical engineering from the Indian Institute of Technology, Kharagpur, in 1995 and the M.S. degree from Boston University, Boston, MA, in 1996. He is currently pursuing the Ph.D. in mechanical engineering at the Massachusetts Institute of Technology, Cambridge, MA.

His research interests include adaptive and nonlinear control theory, and their applications to flight vehicles.

**Clas Jacobson** (S'81–M'82) received the B.S. degree in computer and systems engineering in 1982, and the M.Eng. and Ph.D. degrees in 1984 and 1986, respectively, all from Rensselaer Polytechnic Institute, Troy, NY.

He joined Northeastern University, Boston, MA, in 1986 as an Assistant Professor in the Department of Electrical and Computer Engineering and was promoted to Associate Professor (with tenure) in 1992. He joined United Technologies Research Center (UTRC) in 1995, where he is presently Group Leader for Controls Technology in the Mechatronics Systems Department. His areas of expertise include system identification, adaptive systems, distributed parameter systems, and control of nonlinear dynamical systems.

Dr. Jacobson received UTRC outstanding achievement awards in 1995, 1996, and 1997.